Synthetic Biology **Biotechnology and Bioengineering**
DOI 10.1002/bit.26448

Systematic Optimization of L-Tryptophan Riboswitches for Efficient Monitoring of the Metabolite in *Escherichia coli*†

Running title: Optimization Strategies for Riboswitches

Sungho Jang [1] and Gyoo Yeol Jung [1,2,*]

[1] Department of Chemical Engineering, Pohang University of Science and Technology, 77 Cheongam-ro, Nam-gu, Pohang, Gyeongbuk, 37673, Korea

[2] School of Interdisciplinary Bioscience and Bioengineering, Pohang University of Science and Technology, 77 Cheongam-ro, Nam-gu, Pohang, Gyeongbuk, 37673, Korea

[*] To whom correspondence should be addressed: Gyoo Yeol Jung

E-mail: gyjung@postech.ac.kr

Address: Department of Chemical Engineering, Pohang University of Science and Technology, 77 Cheongam-ro, Nam-gu, Pohang, Gyeongbuk 37673, Korea

Tel.: +82-54-279-2391, Fax: +82-54-279-5528

†This article has been accepted for publication and undergone full peer review but has not been through the copyediting, typesetting, pagination and proofreading process, which may lead to differences between this version and the Version of Record. Please cite this article as doi: [10.1002/bit.26448]

Additional Supporting Information may be found in the online version of this article.

Received June 21, 2017; Revision Received August 11, 2017; Accepted September 8, 2017

ABSTRACT

Riboswitches form a class of genetically-encoded sensor-regulators and are considered as promising tools for monitoring various metabolites. Functional parameters of a riboswitch, like dynamic or operational range, should be optimized before it is implemented in a specific application for monitoring the target molecule efficiently. However, optimization of a riboswitch was not straightforward and required detailed studies owing to its complex sequence-function relationship. Here, we present three approaches for tuning and optimization of functional parameters of a riboswitch using an artificial L-tryptophan riboswitch as an example. First, the constitutive expression level was adjusted to control the dynamic range of an L-tryptophan riboswitch. The dynamic range increased as the constitutive expression level increased. Then, the function of a riboswitch-encoded protein was utilized to connect the regulatory response of the riboswitch to another outcome for amplifying the dynamic range. Riboswitch-mediated control of the host cell growth enabled the amplification of the riboswitch response. Finally, L-tryptophan aptamers with different dissociation constants were employed to alter the operational range of the riboswitch. The dose-response curve was shifted towards higher L-tryptophan concentrations when an aptamer with higher dissociation constant was employed. All strategies were effective in modifying the distinct functional parameters of the L-tryptophan riboswitch, and they could be easily applied to optimization of other riboswitches owing to their simplicity.

Keywords: riboswitch tuning; biosensor; dose-response curve; L-tryptophan; synthetic biology

This article is protected by copyright. All rights reserved

Riboswitches form a class of genetically-encoded biosensors composed exclusively of RNA that regulates gene expression in response to metabolites (Mandal and Breaker, 2004). This RNA switch is composed of two domains—an aptamer that binds to a ligand, and an expression platform, which transforms the binding event into the expression of a gene usually located downstream of the riboswitch. Binding of the ligand to the aptamer causes changes in the secondary and tertiary structures of the riboswitch, influencing translation initiation, transcription termination, or mRNA stability. Owing to the widespread prevalence and the diversity of detectable ligands of natural riboswitches, they were utilized for understanding their molecular interactions and structural dynamics, comprehending cellular metabolism, and validating antimicrobial targets. Furthermore, RNA aptamers, selected *in vitro* by a method called systematic evolution of ligands by exponential enrichment (SELEX), can be employed in combination with rational designs or combinatorial screens to construct artificial riboswitches for new target ligands (Topp and Gallivan, 2010). These artificial riboswitches have been applied for reprogramming of bacterial behavior (Topp and Gallivan, 2007), screening and selection of metabolite producers (Xiu et al., 2017), and generation of orthogonal regulators (Dixon et al., 2012).

Potential of the riboswitches as *in vivo* metabolite sensors has been highlighted because monitoring of metabolite concentration can help various applications and RNA aptamers could be created for almost every molecule in principle (Machtel et al., 2016). To maximize the performance of the riboswitches as metabolite sensors, several requirements should be addressed, which could be described using a dose-response curve (Figure 1A) (Link and Breaker, 2009). First, a riboswitch should discriminate the presence or the absence of a target ligand as clearly as possible. In other words, the difference between the riboswitch responses at non-induced and

fully-induced states, which could be defined as fold activation or dynamic range, should be high enough. Second, the basal expression level of a riboswitch-regulated protein is desired to be minimized. Overexpression of the protein can negatively affect the fitness of the cell which harbors the riboswitch by causing metabolic burden. Finally, the operational range of the riboswitch should be modulated to be matched with the requirements of applications to effectively monitor the change in ligand concentration.

However, optimization of riboswitch function to fulfill the aforementioned requisites is not straightforward due to the complex sequence-function relationship and non-modular nature of riboswitch (Smolke, 2009). The sequence of riboswitch determines not only the binding of a target ligand, but also the switching performance and the expression level of the riboswitch. Consequently, a considerable amount of information, such as about structure and evolutionary relationship, was necessary for successful optimization (Rode et al., 2015). Artificial riboswitches based on non-natural RNA aptamers, however, generally lack such detailed information, and alternative tuning options need to be considered which could be easily adjusted (Figure 1B). Here, we present three strategies for tuning of the dose-response curve of riboswitch using an artificial L-tryptophan riboswitch as an example. First, the effect of the constitutive expression level of the riboswitch was investigated. We modulated the strength of the promoter or the copy number of the plasmid to optimize dynamic range and fold activation of the riboswitch. Then, a riboswitch-regulated protein, *tetA* (a gene encoding H^+/tetracycline antiporter), was utilized to amplify the response of riboswitch by tetracycline supplementation. Finally, an L-tryptophan aptamer, with a different affinity towards the ligand, was employed to construct a variant riboswitch that operates in a distinct range of L-tryptophan concentration.

Initially, an artificial L-tryptophan riboswitch was created by *in vivo* selection (Jang et al., 2015; Muranaka et al., 2009) of a riboswitch library composed of an L-tryptophan aptamer (70–727) (Majerfeld and Yarus, 2005), a randomized linker, a ribosome binding site (RBS), and a selection-screening module (*tetA-sgfp*) (Figure 1B). Although computational designs (Domin et al., 2016; Espah Borujeni et al., 2016) or modular expression platforms (Ceres et al., 2013a; Ceres et al., 2013b) could be utilized for the construction of artificial riboswitches, we chose to take advantage of the *in vivo* selection system because the structural foundation of the L-tryptophan aptamer has not been fully investigated. In this design, binding of L-tryptophan to the aptamer results in expression of the selection-screening module depending on the sequence of the linker (Lynch et al., 2007). The colony with the highest fold activation was chosen after two cycles of dual selection had been performed (see Materials and Methods), and the riboswitch plasmid within the colony was named pAC108_TR727 after its plasmid backbone (pACYCDuet), promoter (BBa_J23108), and aptamer (70-727) (Table S1). This riboswitch activated gene expression by 1.58-fold in the presence of 1 g/L L-tryptophan compared to that when no L-tryptophan was added (Figure S1). We used this riboswitch in the investigation of various options for tuning of riboswitch.

One of the most important characteristics of a metabolite biosensor is its ability to discriminate the presence and the absence of its target molecule. The difference in the response of the biosensor between its basal and fully-induced states, a dynamic range, could be engineered by generating multiple replications of the entire sensing-actuating process (Ang et al., 2013). This approach can amplify the response across the whole range of metabolite concentrations at the same ratio, resulting in the vertical scaling of the dose-response curve. Accordingly, the dynamic range might be enlarged because both basal and fully-induced responses are amplified

at the ratio similar to the increase in the number of the sensing-actuating process. Since the number of the sensing-actuating process is determined by the number of the riboswitch molecules within a cell, we investigated the effect of the constitutive expression level of the riboswitch on its dynamic range. Three variant plasmids were created based on pAC108_TR727 using either synthetic promoters with various strengths (BBa_J23114: 256 a.u., BBa_J23108: 1303 a.u., BBa_J23100: 2547 a.u.) (iGEM Foundation,) or plasmids with different copy numbers (pACYCDuet: 10–12 copies/cell, pCDFDuet: 20–40 copies/cell) to control the number of the mRNA molecules that encode the riboswitch (Figure 2A). When dose-response curves were evaluated for all the variants, a general trend was observed that dynamic ranges were augmented at the cost of increased basal expression levels (Figure 2B). The curves were scaled vertically as the constitutive expression level increased, which is in accordance with our rationale. Additionally, fold activation, the fully-induced expression level divided by the basal expression level, tended to increase as the constitutive expression level increased (Figure 2C). However, the fold activation of pAC100_TR727 was not the highest even at the highest constitutive expression level. This deviation of the fold activation of pAC100_TR727 from the trend could be due to the metabolic burden caused by overexpression of the riboswitch-regulated gene (Muhamadali et al., 2016). Indeed, the optical density at 600 nm ($O.D._{600}$) of the cell, which contained pAC100_TR727, was lower than that of the cell, which contained pAC108_TR727, by 37% when they were fully induced (Figure S2). This trade-off between the dynamic range and the fitness of the cell proposes that there would be an optimal point where both the dynamic range and the fold activation are maximized, while the cell growth is minimally affected. Collectively, the dynamic range of a riboswitch could be readily modulated by controlling the constitutive expression level, and excessive overexpression negatively affects the function of the riboswitch

as well as the physiology of the cell. The tuning strategy shown here is considered simple and widely applicable because promoter and plasmid are highly modular parts that can be adjusted independent of the regulatory mechanism of the riboswitch.

Next, we connected the response of the riboswitch to another output using a function of the riboswitch-regulated gene to amplify the response. In many signal transduction cascades, a small change in the concentration of a signaling molecule results in a large gain of the final response where the initial signal is amplified by the action of a series of enzymes in the cascades (Kholodenko et al., 1997). Similarly, we utilized the function of the riboswitch-regulated gene, *tetA*, to magnify the dynamic range of the riboswitch. Since *tetA* encodes H^+/tetracycline antiporter, the riboswitch can control the resistance of the host cell towards tetracycline in an L-tryptophan-dependent manner. In this case, the final response could be measured as $O.D._{600}$ of the host cell in the presence of tetracycline. When 100 μg/mL tetracycline was added, the $O.D._{600}$ of the cell that contained pAC108_TR727 was 2.96-fold higher when 1 g/L L-tryptophan than when no L-tryptophan was added (Figure 3). Compared to the fold activation of the riboswitch evaluated by its expression level (1.58-fold), connection of the riboswitch response to another output provided an additional opportunity to adjust the dose-response. Moreover, this signal amplification enabled discrimination in the higher concentration range considering that the dose-response curves were saturated at lower concentrations when the expression level of the riboswitch-regulated protein was exploited as a response (Figure S3). In conclusion, utilization of the function of the riboswitch-regulated gene improved the riboswitch function in terms of the fold activation. This strategy could be further extended if we place other genes with different functions, such as transcriptional regulation or metabolite synthesis, under the control of the riboswitch.

Finally, the operational range of the L-tryptophan riboswitch was tuned. *In vivo* quantification of higher concentrations of L-tryptophan is necessary because this amino acid is industrially important and is mostly produced from microbial cell factories (Rodriguez et al., 2014). Riboswitch can help improve the performance of production hosts by facilitating high-throughput screenings (Jang et al., 2016). Theoretical and experimental studies indicated that the operational range of a riboswitch is largely determined by the strength of the interaction between the aptamer and the ligand of the riboswitch (Beisel and Smolke, 2009; Rode et al., 2015). Therefore, we created an additional L-tryptophan riboswitch to alter the operational range using 70–585 aptamer, which has a lower affinity to the ligand, than that of 70–727 aptamer. Dissociation constants of 70–727 and 70–585 aptamers were 13 and 24.5 μM, respectively (Majerfeld and Yarus, 2005). We performed an *in vivo* selection of a new riboswitch library made from the 70-585 aptamer, because specific interactions between an aptamer and a linker were critical for the function of an artificial riboswitch which employed the similar architecture as used in this study (Lynch et al., 2007). The library was subjected to the dual selection process using *tetA*, same as previously applied for the development of the pAC108_TR727 riboswitch. As a result, we obtained a riboswitch named pAC108_TR585 whose fold activation was 1.58. There were five point mutations clustered near the linker region (Figure S4), which did not abolish L-tryptophan-dependent activation of gene expression. Dose-response curves of pAC108_TR727 and pAC108_TR585 were fitted using their specific fluorescence in the presence of L-tryptophan at various concentrations (Figure 4). The dose-response curve of pAC108_TR585 was shifted toward higher L-tryptophan concentrations than that of pAC108_TR727 did. Half maximal effective concentration (EC_{50}) of pAC108_TR585 was also increased 3.22-fold in comparison with that of pAC108_TR727 (Figure 4, inset). Therefore, the

operational range was successfully modified using an aptamer with a different affinity to the ligand. Although it is not straightforward to rationally engineer the aptamer affinity, combinatorial approaches can assist the development of aptamers with diverse affinities by optimizing the selection conditions (Carothers et al., 2010) or characterizing multiple aptamers in a massively parallel way (Cho et al., 2013). Additionally, selection of RNA aptamers with *in vivo* functionality can be facilitated using structural motifs from natural riboswitches as scaffolds (Porter et al., 2017), because intracellular environment strongly affects proper folding of aptamers and regulation of riboswitch (Marcano-Velázquez and Batey, 2015). Finally, aptamers with different binding affinities could be coupled to modular expression platforms (Ceres et al., 2013a) to accelerate the optimization of riboswitches.

In conclusion, we demonstrated a systematic optimization of the various functional parameters of L-tryptophan riboswitches. Dynamic range of the riboswitch was readily adjusted using modular parts, which are independent of the mechanism of the riboswitch. Additionally, the existence of an optimal expression level was suggested. Utilization of the function of the riboswitch-encoded protein further increased the fold activation of the response. Finally, the operational range was modulated using aptamers with different affinities. The tuning strategies presented in this work could be applied to many riboswitches as various parts for each option are being developed.

MATERIALS AND METHODS

Bacterial strains, plasmids, and reagents

The *Escherichia coli* strains and plasmids used in this study are listed in Table S1. The DNA oligonucleotides were synthesized by Bioneer (Daejeon, Korea) and are listed in Table S2.

Q5 DNA polymerase, T4 DNA ligase, and restriction endonucleases were purchased from New England Biolabs (Ipswich, MA, USA). Sequencing of the plasmids was done by Cosmogenetech (Seoul, Korea). All other reagents were obtained from Sigma-Aldrich (St. Louis, MO, USA) unless otherwise indicated.

Measurements of the optical density and the fluorescence

$O.D._{600}$ of the culture broth was measured using either the UV-1700 spectrophotometer (Shimadzu, Japan) or BioscreenC (Oy Growth Curves Ab, Finland). The fluorescence intensity of the culture broth was measured using VICTOR^3 (PerkinElmer) using 486-nm excitation filter and 535-nm emission filter with 1 s measurement time. All cultivations in broth were performed at 37°C under shaking conditions (200 rpm).

***In vivo* selection of L-tryptophan riboswitches**

The pTrpRibo plasmid was PCR-amplified using TrpRS_F and TrpRS_R as primers, subcloned into the pACYCDuet using *Asc*I and *Not*I, and transformed into Mach-T1^R competent cells to construct pTrpTemplate. The riboswitch libraries were prepared by PCR amplification of the pTrpTemplate using Lib_F and 727_Library_R or 585_Library_R as primers. The PCR products were separately ligated using T4 DNA ligase and transformed into the MegaX DH10B electrocompetent cells (Invitrogen). After an incubation at 37°C for 8 h on Luria Bertani agar plate with 34 µg/mL chloramphenicol (CLB), about 10^7 colonies were harvested and plasmids were extracted using Exprep Plasmid SV kit (GeneAll Biotechnology, Seoul, Korea).

L-Tryptophan riboswitches were selected *in vivo* using *tetA* as a dual selectable marker (Nomura and Yokobayashi, 2007a; Nomura and Yokobayashi, 2007b; Sharma et al., 2008). *E. coli* W3110 cells were transformed with the riboswitch plasmid libraries and incubated at 37°C

on a CLB-agar plate. The colonies were collected and washed three times using M9 minimal medium (1× M9 salts, 2 mM $MgSO_4$, 0.1 mM $CaCl_2$, and 4 g/L glucose) with 34 μg/mL chloramphenicol (CM9). The cells were inoculated into 3 mL CM9 at an $O.D._{600}$ of 0.05 and incubated until $O.D._{600}$ reached 0.5. For negative selection, the culture broth was diluted to 3 mL CM9 with 0.4 mM $NiCl_2$ at an $O.D._{600}$ of 0.01 and incubated until $O.D._{600}$ reached 0.5. Then, the culture broth was washed three times with fresh CM9, inoculated into 3 mL CM9 with 0.2 g/L L-tryptophan at an $O.D._{600}$ of 0.05, and incubated until $O.D._{600}$ reached 0.5. Then, for positive selection, the culture broth was diluted with 3 mL CM9 with 0.2 g/L L-tryptophan and 40 μg/mL tetracycline at an $O.D._{600}$ of 0.01 and incubated until $O.D._{600}$ reached 0.5. Two cycles of dual selections (negative selection followed by positive selection) were performed for each library. The culture broth was spread onto a CLB-agar plate. Several colonies were cultured in CM9 with or without 0.2 g/L L-tryptophan. Fluorescence of the culture broths was normalized by their $O.D._{600}$ to calculate specific fluorescence. The fold activation was evaluated by normalizing the specific fluorescence with 0.2 g/L L-tryptophan to that with no L-tryptophan. A colony with the highest fold activation was chosen from each library, and the riboswitches in those colonies were named pAC108_TR727 and pAC108_TR585.

Construction of the riboswitch variants

The constitutive expression level of pAC108_TR727 was adjusted by changing the promoter or the vector. pAC108_TR727 was PCR-amplified with TrpRS_R and either J23100_F or J23114_F and subcloned into pACYCDuet to create pAC100_TR727 or pAC114_TR727, respectively. Additionally, pAC108_TR727 was digested with *Asc*I and *Not*I and cloned into the same sites in pCDFDuet to construct pCD108_TR727.

Evaluation of dose-responses of the riboswitches

Single colonies of the *E. coli* strains that contained riboswitches were inoculated into 3 mL CM9 and cultured overnight. The culture broths were refreshed by diluting them in 3 mL fresh CM9 at an $O.D._{600}$ of 0.05 and incubated for 6 h. Then, the culture broths were inoculated into 200 μL CM9 with various concentrations of L-tryptophan (0, 0.001, 0.003, 0.01, 0.03, 0.1, 0.3, and 1 g/L) at an $O.D._{600}$ of 0.05 and incubated in BioscreenC plates. $O.D._{600}$ and fluorescence intensity were measured after 6 h to calculate the specific fluorescence. The dose-response curves of the riboswitches were fitted using the following equation: Specific fluorescence = Minimum + (Maximum − Minimum) / $(1 + 10^{(\log(EC50) - \log(L\text{-}Trp))})$. The EC_{50}s of the riboswitches were estimated from the fitting results. The response of the riboswitch-containing *E. coli* strain towards tetracycline was tested by supplementing tetracycline at 100 μg/mL after 1-h adaptation period and $O.D._{600}$ was measured after 9 h. All the cultures were performed in biological triplicates.

ACKNOWLEDGEMENTS

This work was supported by the Global Research Laboratory Program (NRF-2016K1A1A2912829) and the C1 Gas Refinery Program (NRF-2016M3D3A1A01913237) through the National Research Foundation of Korea (NRF) funded by the Korea Government (Ministry of Science, ICT & Future Planning).

CONFLICT OF INTEREST

The authors declare no competing financial interest.

REFERENCES

Ang J, Harris E, Hussey BJ, Kil R, McMillen DR. 2013. Tuning response curves for synthetic biology. ACS Synth Biol 2:547–567.

Beisel CL, Smolke CD. 2009. Design principles for riboswitch function. PLoS Comput Biol 5:e1000363.

Carothers JM, Goler JA, Kapoor Y, Lara L, Keasling JD. 2010. Selecting RNA aptamers for synthetic biology: investigating magnesium dependence and predicting binding affinity. Nucleic Acids Res 38:2736–2747.

Ceres P, Garst AD, Marcano-Velázquez JG, Batey RT. 2013a. Modularity of select riboswitch expression platforms enables facile engineering of novel genetic regulatory devices. ACS Synth Biol 2:463–472.

Ceres P, Trausch JJ, Batey RT. 2013b. Engineering modular "ON" RNA switches using biological components. Nucleic Acids Res 41:10449–10461.

Cho M, Soo Oh S, Nie J, Stewart R, Eisenstein M, Chambers J, Marth JD, Walker F, Thomson JA, Soh HT. 2013. Quantitative selection and parallel characterization of aptamers. Proc Natl Acad Sci U S A 110:18460–18465.

Dixon N, Robinson CJ, Geerlings T, Duncan JN, Drummond SP, Micklefield J. 2012. Orthogonal riboswitches for tuneable coexpression in bacteria. Angew Chem Int Ed 51:3620–3624.

Domin G, Findeiß S, Wachsmuth M, Will S, Stadler PF, Mörl M. 2016. Applicability of a computational design approach for synthetic riboswitches. Nucleic Acids Res 45:4108-4119.

Espah Borujeni A, Mishler DM, Wang J, Huso W, Salis HM. 2016. Automated physics-based design of synthetic riboswitches from diverse RNA aptamers. Nucleic Acids Res 44:1–13.

iGEM Foundation. Anderson series promoters. Registry of Standard Biological Parts. http://parts.igem.org/Promoters/Catalog/Constitutive.

Jang S, Lee B, Jeong H-H, Jin SH, Jang S, Kim SG, Jung GY, Lee C-S. 2016. On-chip analysis, indexing and screening for chemical producing bacteria in a microfluidic static droplet array. Lab Chip 16:1909–1916.

Jang S, Yang J, Seo SW, Jung GY. 2015. Riboselector: riboswitch-based synthetic selection device to expedite evolution of metabolite-producing microorganisms. Methods Enzymol 550:341–362.

Kholodenko BN, Hoek JB, Westerhoff HV, Brown GC. 1997. Quantification of information transfer via cellular signal transduction pathways. FEBS Lett 414:430–434.

Link KH, Breaker RR. 2009. Engineering ligand-responsive gene-control elements: lessons learned from natural riboswitches. Gene Ther 16:1189–1201.

Lynch SA, Desai SK, Sajja HK, Gallivan JP. 2007. A high-throughput screen for synthetic riboswitches reveals mechanistic insights into their function. Chem Biol 14:173–184.

Machtel P, Bąkowska-Żywicka K, Żywicki M. 2016. Emerging applications of riboswitches - from antibacterial targets to molecular tools. J Appl Genet 57:531–541.

Majerfeld I, Yarus M. 2005. A diminutive and specific RNA binding site for L-tryptophan. Nucleic Acids Res 33:5482–5493.

Mandal M, Breaker RR. 2004. Gene regulation by riboswitches. Nat Rev Mol Cell Biol 5:451–463.

Marcano-Velázquez JG, Batey RT. 2015. Structure-guided mutational analysis of gene regulation by the Bacillus subtilis pbuE adenine-responsive riboswitch in a cellular context. J Biol Chem 290:4464–4475.

Muhamadali H, Xu Y, Morra R, Trivedi DK, Rattray NJW, Dixon N, Goodacre R. 2016. Metabolomic analysis of riboswitch containing E. coli recombinant expression system. Mol Biosyst 12:350–361.

Muranaka N, Sharma V, Nomura Y, Yokobayashi Y. 2009. An efficient platform for genetic selection and screening of gene switches in Escherichia coli. Nucleic Acids Res 37:e39.

Nomura Y, Yokobayashi Y. 2007a. Dual selection of a genetic switch by a single selection marker. BioSystems 90:115–120.

Nomura Y, Yokobayashi Y. 2007b. Reengineering a natural riboswitch by dual genetic selection. J Am Chem Soc 129:13814–13815.

Porter EB, Polaski JT, Morck MM, Batey RT. 2017. Recurrent RNA motifs as scaffolds for genetically encodable small-molecule biosensors. Nat Chem Biol 13:295–301.

Rode AB, Endoh T, Sugimoto N. 2015. Tuning riboswitch-mediated gene regulation by rational control of aptamer ligand binding properties. Angew Chem Int Ed 54:905–909.

Rodriguez A, Martínez JA, Flores N, Escalante A, Gosset G, Bolivar F. 2014. Engineering Escherichia coli to overproduce aromatic amino acids and derived compounds. Microb Cell Fact 13:126.

Sharma V, Nomura Y, Yokobayashi Y. 2008. Engineering complex riboswitch regulation by dual genetic selection. J Am Chem Soc 130:16310–16315.

Smolke C ed. 2009. The metabolic pathway engineering handbook: tools and applications. CRC Press.

Topp S, Gallivan JP. 2007. Guiding bacteria with small molecules and RNA. J Am Chem Soc 129:6807–6811.

Topp S, Gallivan JP. 2010. Emerging applications of riboswitches in chemical biology. ACS Chem Biol 5:139–148.

Xiu Y, Jang S, Jones JA, Zill NA, Linhardt RJ, Yuan Q, Jung GY, Koffas MAG. 2017. Naringenin-responsive riboswitch-based fluorescent biosensor module for Escherichia coli co-cultures. Biotechnol Bioeng.

FIGURE LEGENDS

Figure 1. Strategies for tuning of the dose-response of riboswitches. (A) A typical dose-response curve of an activation type riboswitch. Following parameters describe the characteristics of the riboswitch. BE: basal expression level; FA: fold activation; DR: dynamic range; OR: operational range; EC_{50}: half maximal effective concentration. (B) Tuning options for modulation of the riboswitch function.

Figure 2. Effect of the constitutive expression level on the riboswitch function. (A) Construction of the variant constructs using synthetic promoters and different plasmids for controlling the constitutive expression level. (B) Dose-response curves of the variant constructs. (C) Fold activations of the variant constructs. Specific fluorescence with 1 g/L L-tryptophan was normalized to that when no L-tryptophan was added to calculate the fold activation. P-values were obtained from the t-tests: * $P < 0.05$; ** $P < 0.005$; *** $P < 0.001$. The fold activation of pAC100_TR727 showed no statistical significance when compared with the other riboswitch constructs. Error bars indicate standard deviations from three biological replicates.

Figure 3. Amplification of the dynamic range using the function of *tetA*. $O.D._{600}$ of the *E. coli* strain containing pAC108_TR727 with various concentrations of L-tryptophan was normalized to that when no L-tryptophan was added to calculate fold activations. Error bars indicate standard deviations from three biological replicates.

Figure 4. Development of L-tryptophan riboswitches with distinct operational ranges using aptamers with different binding affinities. Dose-response curves were evaluated using specific fluorescence with various concentrations of L-tryptophan. Error bars indicate

standard deviations from three biological replicates. Inset: EC_{50} values of the riboswitches. Error bars indicate standard errors from three biological replicates.

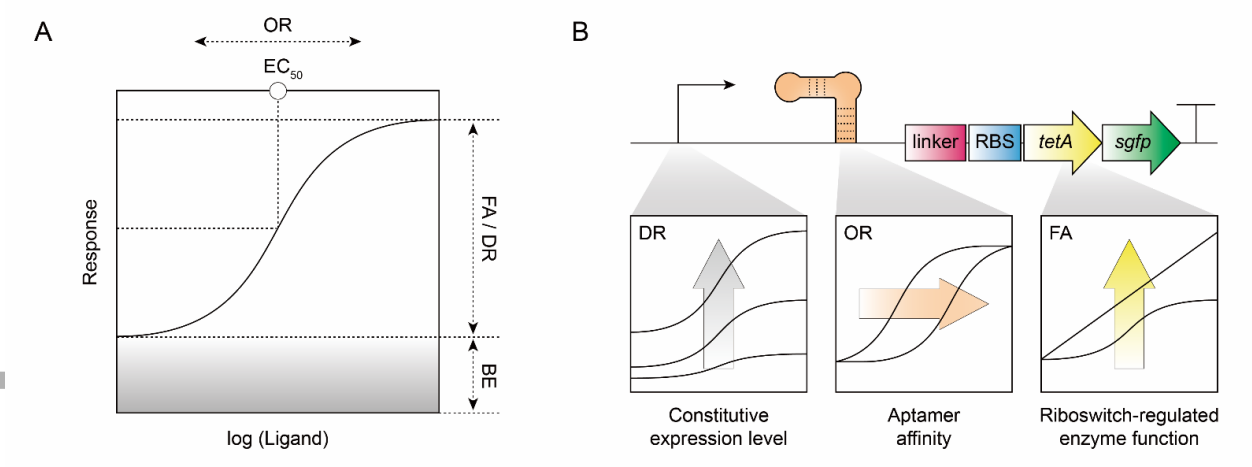

Figure 1

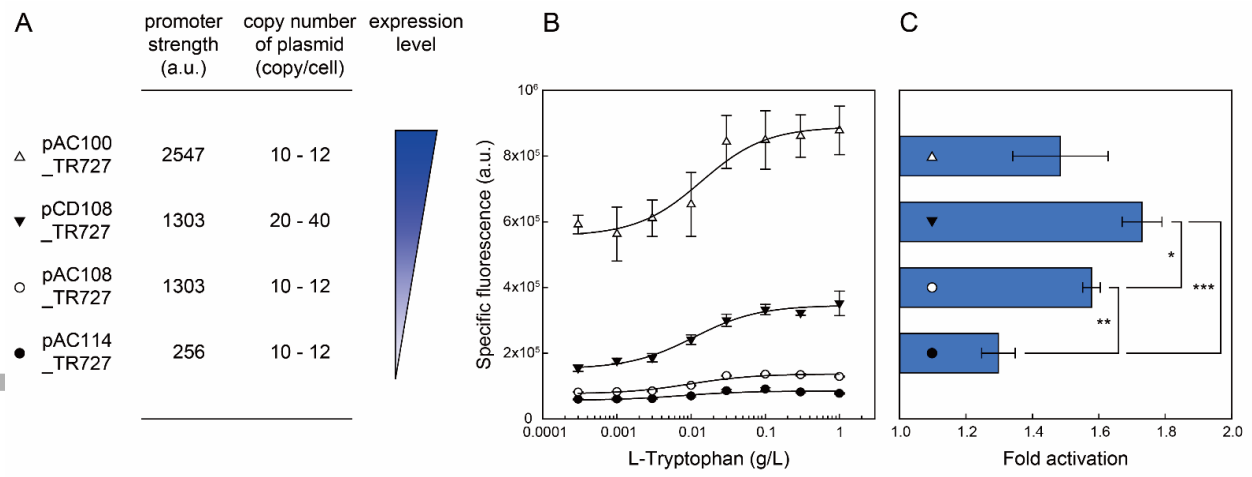

Figure 2

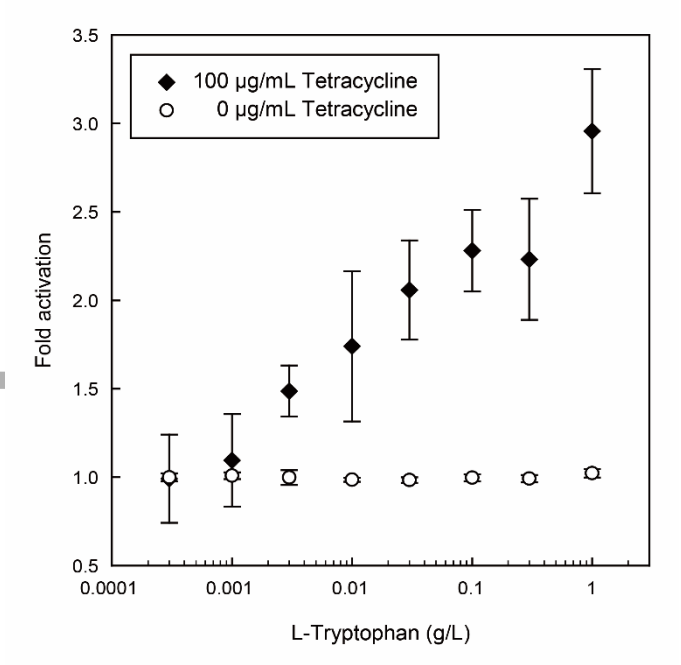

Figure 3

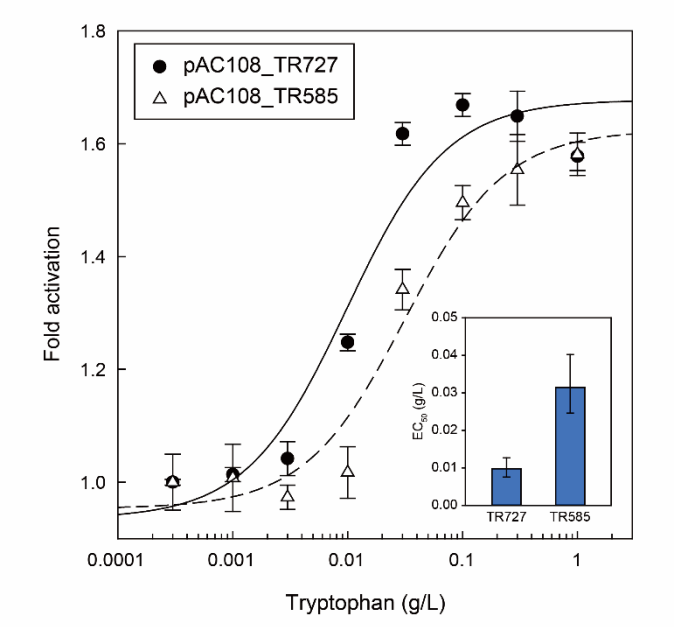

Figure 4